Improving the Laplace transform integration method

Peter Lynch* and Colm Clancy
School of Mathematics and Statistics, University College Dublin, Ireland

Abstract

We consider the Laplace transform filtering integration scheme applied to the shallow water equations, and demonstrate how it can be formulated as a finite difference scheme in the time domain. In addition, we investigate a more accurate treatment of the nonlinear terms. The advantages of the resulting algorithms are demonstrated by means of numerical integrations.

1 Introduction

In Clancy and Lynch (2011), hereafter CL11, a time integration scheme based on a modified inversion to the Laplace transform (LT) was applied to a spectral shallow water model. The scheme is designed to permit long time-steps for integrations and to filter out unwanted high frequencies. In terms of stability and accuracy, it was generally found to compare favourably with the widely-used semi-implicit method (Kwizak and Robert, 1971). The LT scheme had the additional benefit of reduced phase error, which is a feature of the trapezoidal averaging in the semi-implicit approach.

In this note, we describe two improvements to the LT algorithm. We show how, in certain models, we can formulate it as a scheme in the time domain without any explicit computations in the domain of the complex transform variable. We also consider a more accurate treatment of the nonlinear terms in the discretised model and compare with the scheme of CL11.

2 The Laplace transform integration method

We begin with a general dynamical system, which may arise after the spatial discretisation of the equations governing a given atmospheric model:

$$\frac{\mathrm{d}\mathbf{X}}{\mathrm{d}t} = \mathbf{L}\,\mathbf{X} + \mathbf{N}(\mathbf{X}) \tag{1}$$

Here $\mathbf{X}$ is the state vector and we have split the right-hand side forcing into linear and nonlinear terms. We take the Laplace transform of this system, making use of the properties given in (10) in the appendix. As in CL11, we first consider the transform over the interval $[(\tau-1)\,\Delta t, (\tau+1)\,\Delta t]$: the 'initial condition' is then given by $\mathbf{X}^{\tau-1}$ and the nonlinear terms are evaluated at the centre value $\mathbf{N}^{\tau} \equiv \mathbf{N}(\mathbf{X}^{\tau})$. Thus, we have

$$s\,\widehat{\mathbf{X}} - \mathbf{X}^{\tau-1} = \mathbf{L}\,\widehat{\mathbf{X}} + \frac{1}{s}\,\mathbf{N}^{\tau} \tag{2}$$

*Peter.Lynch@ucd.ie

Rearranging, we have an equation for the transform:

$$\widehat{\mathbf{X}}(s) = (s\mathbf{I} - \mathbf{L})^{-1} \left[\mathbf{X}^{\tau-1} + \frac{1}{s} \mathbf{N}^{\tau} \right] \tag{3}$$

The physical solution is recovered by applying an inverse transform. As described in the appendix, a modified inversion operator may be used to filter components with frequencies larger than a cut-off ω_c. This operator, $\mathfrak{L}^*$, involves a complex integral around a circle. In CL11, a discretised form of the operator was used, denoted by $\mathfrak{L}^*_N$ and defined in (14) below. Using this we get the solution:

$$\mathbf{X}^{\tau+1} = \mathfrak{L}^*_N \left\{ \widehat{\mathbf{X}}(s) \right\} = \frac{1}{N} \sum_{n=1}^{N} e_N^{s_n \, 2\Delta t} \widehat{\mathbf{X}}(s_n) \, s_n \tag{4}$$

Together, equations (3) and (4) define a time-stepping scheme, which may be applied to any dynamical system of the form (1).

In the context of atmospheric models, the $(s\mathbf{I} - \mathbf{L})^{-1}$ term in (3) corresponds to an elliptic equation which would need to be solved at each of the points s_n, $n = 1, \ldots, N$; as an example, Lynch (1991) used $N = 8$. This extra computational effort motivated the use of a spectral transform model in CL11, in which the solution of the elliptic equation reduces to multiplication by constants in spectral space. In the next section, we will outline some further improvements on this approach.

3 Improvements to the time scheme

3.1 Spectral model

The shallow water equations may be written in the form

$$\begin{aligned} \frac{\partial \eta}{\partial t} &= -\nabla . (\eta \mathbf{V}) \\ \frac{\partial \delta}{\partial t} + \nabla^2 \Phi &= \mathbf{k} . \nabla \times (\eta \mathbf{V}) - \nabla^2 \left(\frac{\mathbf{V} . \mathbf{V}}{2(1-\mu^2)} \right) \\ \frac{\partial \Phi'}{\partial t} + \bar{\Phi} \delta &= -\nabla . \left[(\Phi' - \Phi_s) \, \mathbf{V} \right] \end{aligned} \tag{5}$$

Here η is the absolute vorticity, δ is the horizontal divergence, $\mathbf{V}$ is the horizontal wind vector and μ is the sine of latitude. The free surface geopotential height has been written as $\Phi = \bar{\Phi} + \Phi'$, where $\bar{\Phi}$ is constant. The geopotential of the orography is given by Φ_s.

In CL11, the equations were discretised using the spectral transform model of Hack and Jakob (1992), in which the fields are expanded as truncated series of spherical harmonics; for example, with a triangular truncation,

$$\eta(\lambda, \mu, t) = \sum_{\ell=0}^{L} \sum_{m=-\ell}^{\ell} \eta_\ell^m(t) e^{im\lambda} P_\ell^m(\mu)$$

For the spectral transform method, the nonlinear terms on the right-hand side of (5) are computed in physical space and the product is expanded in a series. Orthogonality of the spherical harmonics

can then be used to obtain a series of equations for the spectral coefficients. We are left with a set of ordinary differential equations of the form

$$\begin{aligned}\frac{\mathrm{d}}{\mathrm{d}t}\eta_\ell^m &= \mathcal{N}_\ell^m \\ \frac{\mathrm{d}}{\mathrm{d}t}\delta_\ell^m &= \frac{\ell(\ell+1)}{a^2}\,\Phi_\ell^m + \mathcal{D}_\ell^m \\ \frac{\mathrm{d}}{\mathrm{d}t}\Phi_\ell^m &= -\bar{\Phi}\,\delta_\ell^m + \mathcal{F}_\ell^m\end{aligned} \tag{6}$$

where $\mathcal{N}_\ell^m$, $\mathcal{D}_\ell^m$ and $\mathcal{F}_\ell^m$ are the spectral coefficients of the nonlinear terms. Note that the Φ_ℓ^m are the spectral coefficients of the perturbation geopotential Φ'; the prime has been dropped for ease of notation.

We now take the LT of the system (6), as described in Section 2 above. The resulting decoupled system can be solved to give

$$\begin{aligned}\widehat{\eta_\ell^m} &= \frac{1}{s}\,\{\eta_\ell^m\}^{\tau-1} + \frac{1}{s^2}\,\{\mathcal{N}_\ell^m\}^\tau \\ \widehat{\delta_\ell^m} &= d\left(s\{\delta_\ell^m\}^{\tau-1} + \mathcal{R} + \frac{1}{s}\frac{\ell(\ell+1)}{a^2}\{\mathcal{F}_\ell^m\}^\tau\right) \\ \widehat{\Phi_\ell^m} &= d\left(s\,\{\Phi_\ell^m\}^{\tau-1} + \mathcal{Q} - \frac{1}{s}\bar{\Phi}\,\{\mathcal{D}_\ell^m\}^\tau\right)\end{aligned} \tag{7}$$

where

$$\begin{aligned}d &= \frac{1}{s^2+\omega_\ell^2} \\ \mathcal{R} &= \{\mathcal{D}_\ell^m\}^\tau + \frac{\ell(\ell+1)}{a^2}\{\Phi_\ell^m\}^{\tau-1} \\ \mathcal{Q} &= \{\mathcal{F}_\ell^m\}^\tau - \bar{\Phi}\{\delta_\ell^m\}^{\tau-1}\end{aligned}$$

and $\omega_\ell = \sqrt{\ell(\ell+1)\bar{\Phi}/a^2}$ is the frequency of the ℓ-th gravity mode (cf. CL11, Eqn. (15) rewritten in a different form).

In CL11, we used the inversion operator $\mathfrak{L}_N^*$ to compute the spectral coefficients at the new time $(\tau+1)\,\Delta t$, which is at a time $2\,\Delta t$ after the beginning of the time interval. However, by inspection of the form of (7), it is apparent that we can apply the analytical operator $\mathfrak{L}^*$, as defined in (12) in the appendix, to obtain the solution.[1] The right-hand side of the vorticity equation has poles at the origin, so it inverts to

$$\{\eta_\ell^m\}^{\tau+1} = \{\eta_\ell^m\}^{\tau-1} + 2\Delta t\{\mathcal{N}_\ell^m\}^\tau$$

This is equivalent to the conventional leapfrog scheme.

The divergence and continuity equations have poles at $s=0$ and also at $s=\pm i\omega_\ell$. Depending on whether $\omega_\ell < \omega_\mathrm{c}$ or $\omega_\ell > \omega_\mathrm{c}$, these are within or outside the contour $\mathcal{C}^*$. We can use the identities

[1] Nick Byrne, personal communication.

in (13) below to write the solutions as

$$\begin{aligned}
\{\delta_\ell^m\}^{\tau+1} &= H(\omega_\ell)\cos(2\omega_\ell\Delta t)\,\{\delta_\ell^m\}^{\tau-1} \\
&\quad + \frac{1}{\omega_\ell}H(\omega_\ell)\sin(2\omega_\ell\Delta t)\,\mathcal{R} \\
&\quad + \frac{1}{\omega_\ell^2}\left[(1-H(\omega_\ell)\cos(2\omega_\ell\Delta t)\right]\frac{\ell(\ell+1)}{a^2}\{\mathcal{F}_\ell^m\}^\tau \qquad (8)\\
\{\Phi_\ell^m\}^{\tau+1} &= H(\omega_\ell)\cos(2\omega_\ell\Delta t)\,\{\Phi_\ell^m\}^{\tau-1} \\
&\quad + \frac{1}{\omega_\ell}H(\omega_\ell)\sin(2\omega_\ell\Delta t)\,\mathcal{Q} \\
&\quad - \frac{1}{\omega_\ell^2}\left[(1-H(\omega_\ell)\cos(2\omega_\ell\Delta t)\right]\frac{\ell(\ell+1)}{a^2}\bar{\Phi}\{\mathcal{D}_\ell^m\}^\tau \qquad (9)
\end{aligned}$$

The system (8)–(9) provides a means of advancing the integration without any explicit computations in the complex s-plane. It is simpler than the method discussed in CL11, and avoids the errors associated with the numerical inversion using $\mathfrak{L}_{\mathrm{N}}^*$.

There is a further benefit of analytical inversion, relating to stability. Equation (10) of CL11 gives a stability criterion for the LT discretisation, which may be limiting for large ω_c and small values of N. Using the analytic inversion, i.e. $N \to \infty$, removes this constraint. Stability is then governed by the condition associated with the discretisation of the nonlinear terms.

3.2 Nonlinear terms

Until now, we have been using a leapfrog scheme, in which the nonlinear terms are treated at their centred values; c.f. the discretisation in (2). The three time levels used in the leapfrog introduces a spurious computational mode. Traditionally, when using the semi-implicit leapfrog scheme, a time filter has been added to suppress this noise (Asselin, 1972), although this is known to cause a reduction in accuracy (Williams, 2011).

We would like to have a more accurate treatment of nonlinear terms in the LT scheme. A number of single-stage methods were tested, including a third-order Adams-Bashforth scheme. Durran (1991) previously showed that this scheme is unstable when coupled with a trapezoidal averaging of the linear terms in a semi-implicit. This also proved to be the case when coupled with the LT approach.

Clancy and Pudykiewicz (2013a) tested a number of two-stage semi-implicit methods, in which the nonlinear terms are discretised in time using a predictor–corrector method. One in particular, labelled T-ABT, uses an implicit trapezoidal (T) averaging for the linear terms, with an Adams-Bashforth-Trapezoidal (ABT) method (Kar, 2012) for the nonlinear terms. With $\mathbf{X}^p$ denoting the intermediate, predicted level, the discretisation for the system (1) is then

$$\begin{aligned}
\frac{\mathbf{X}^p - \mathbf{X}^\tau}{\Delta t} &= \frac{1}{2}\mathbf{L}\mathbf{X}^p + \frac{1}{2}\mathbf{L}\mathbf{X}^\tau + \frac{3}{2}\mathbf{N}^\tau - \frac{1}{2}\mathbf{N}^{\tau-1} \\
\frac{\mathbf{X}^{\tau+1} - \mathbf{X}^\tau}{\Delta t} &= \frac{1}{2}\mathbf{L}\mathbf{X}^{\tau+1} + \frac{1}{2}\mathbf{L}\mathbf{X}^\tau + \frac{1}{2}\mathbf{N}^p + \frac{1}{2}\mathbf{N}^\tau
\end{aligned}$$

Although this is also a three time-level scheme, the computational mode is heavily damped and a filter is not needed.

We can use this approach in the LT scheme. For the predictor stage, the LT of system (1) is given by

$$s\,\widehat{\mathbf{X}} - \mathbf{X}^{\tau} = \mathbf{L}\,\widehat{\mathbf{X}} + \frac{1}{s}\left[\frac{3}{2}\mathbf{N}^{\tau} - \frac{1}{2}\mathbf{N}^{\tau-1}\right]$$

As usual, we solve for $\widehat{\mathbf{X}}$ and invert to get $\mathbf{X}^{p}$. The second, corrector stage is then

$$s\,\widehat{\mathbf{X}} - \mathbf{X}^{\tau} = \mathbf{L}\,\widehat{\mathbf{X}} + \frac{1}{s}\left[\frac{1}{2}\mathbf{N}^{p} + \frac{1}{2}\mathbf{N}^{\tau}\right]$$

Again, we solve and invert to give the solution $\mathbf{X}^{\tau+1}$.

4 Numerical tests

The various time integration schemes will now be tested in the spectral transform model described in the previous section. As mentioned, the model is based on that of Hack and Jakob (1992) used in CL11. Here we use a version written in Matlab, using the spectral routines of Drake and Guo (2001).

All cases shown use a T119 spectral resolution, corresponding to a grid of approximately 110km at the equator. The time-step used throughout is 900 s. Three different LT schemes are tested: the original from CL11 using a numerical inversion with $N = 8$; the new version with the analytic transform; and the LT with the ABT treatment of the nonlinear terms, denoted LT-ABT, as described in the previous section. The analytic inversion is also used in the LT-ABT. For comparison, results with the semi-implicit T-ABT are also shown.

We focus on two test cases. The first is described in Läuter et al. (2005) consists of an unsteady flow which has an analytic solution. The horizontal winds and geopotential are given by

$$\begin{aligned}
u(\lambda,\phi,t) =& u_0(\sin\theta\sin\phi\,(\cos\lambda\cos\Omega t - \sin\lambda\sin\Omega t) + \cos\theta\cos\phi)\\
v(\lambda,\phi,t) =& -u_0\sin\theta\,(\sin\lambda\cos\Omega t + \cos\lambda\sin\Omega t)\\
\Phi(\lambda,\phi,t) =& -\frac{1}{2}[u_0(\sin\theta\cos\phi\,(-\cos\lambda\cos\Omega t + \sin\lambda\sin\Omega t)\\
&+ \cos\theta\sin\phi) + a\Omega\sin\phi]^2 + \frac{1}{2}\,(a\Omega\sin\phi)^2 + k_1\\
\Phi_s(\lambda,\phi,t) =& \frac{1}{2}\,(a\Omega\sin\phi)^2 + k_2
\end{aligned}$$

Here a and Ω are the Earth's radius and angular velocity. As in Clancy and Pudykiewicz (2013a), we take $u_0 = 2\pi a/12$ (one circuit of the Earth in twelve days), and choose parameter values $k_1 = 133681\mathrm{m}^2\mathrm{s}^{-2}$, $k_2 = 10\mathrm{m}^2\mathrm{s}^{-2}$ and $\theta = \pi/4$.

In Figure 1 we show the normalised ℓ_∞ height errors over 10 simulated days. For the LT schemes, the cut-off frequency ω_c corresponds to a period of 1 hour. The solutions from the leapfrog-based LT schemes are almost identical, regardless of whether we use a numerical or analytic inversion. Moving away from the leapfrog to the LT-ABT, there is a dramatic improvement and this scheme shows better scores than the T-ABT.

The second case we consider is Case 5 of the suite of Williamson et al. (1992), consisting of zonal flow interacting with an isolated mountain. As this case has no known analytic solution, we compute errors relative to a reference solution from an explicit third-order Adams-Bashforth scheme with $\Delta t = 90$s. The results are shown in Figure 2. On the left we have the same cut-off as

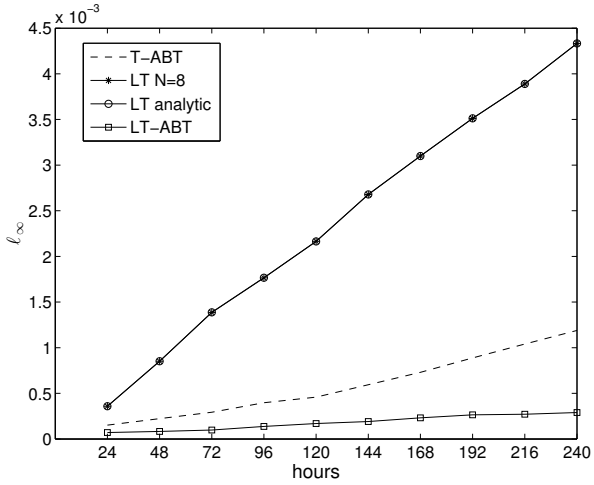

Figure 1: Normalised ℓ_∞ errors for the unsteady flow case. The cut-off period for the LT schemes is 1 hour.

before for the LT algorithms, corresponding to a 1 hour period. On the right, a 3 hour period is used. In this test, we also run the LT with an $N = 16$ numerical inversion.

In general, the LT solutions outperform the semi-implicit here but differences between the various schemes appear with the longer 3-hour cut-off. This corresponds to a lower cut-off frequency ω_c; i.e. the radius of the contour for inversion with $\mathfrak{L}^*$ is smaller and we are filtering more frequencies. The analytic inversion has a sharp, step-function filter response, whereas the response of the numerical inversion (given by (15) in the appendix) distorts modes near the cut-off. Referring again to the right-hand panel of Figure 2, this effect is clearly lessened when N is increased to 16, and disappears in the analytic cases.

5 Discussion

In this note we have outlined some improvements to the Laplace transform time integration scheme developed in Clancy and Lynch (2011) and tested these modifications with numerical simulations. In the original formulation of the LT scheme, we used a numerical inversion to compute the physical solution. Here, in a spectral transform shallow water model, we have shown that this may be replaced by an analytic inversion, thus requiring no explicit integration in the complex transform space. Tests with the model show improved results.

One important advantage of the LT method of time integration is the more accurate phase speed of the linear modes. The analysis of CL11 showed the phase error to be $O(\Delta t^N)$, compared with $O(\Delta t^2)$ for a trapezoidal discretisation used in semi-implicit schemes. The analytic inversion represents the $N \to \infty$ limit. In this case we have exact treatment of linear modes and the algorithm is among a class of exponential integration methods (Beylkin et al., 1998; Clancy and Pudykiewicz, 2013b).

The approach described in this study will not always be practical, because it requires a sim-

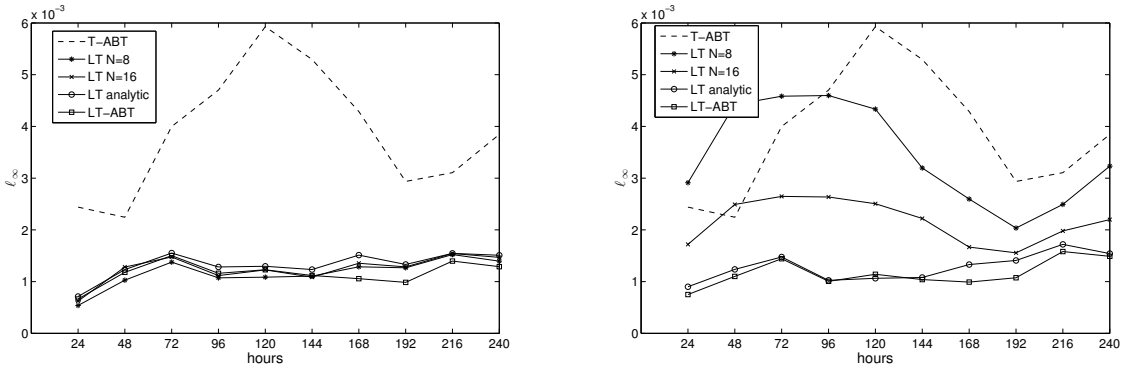

Figure 2: Normalised ℓ_∞ errors for the mountain case. The cut-off period for the LT schemes is 1 hour (left) and 3 hours (right).

ple representation of the linear terms; c.f. Daley (1980), who used a similar time scheme after diagonalising with a normal mode decomposition. However, it is particularly convenient for application to spectral and pseudo-spectral Eulerian models. The numerical experiments show that we can increase the accuracy with a better treatment of the nonlinear terms; previously these were discretised with a centred, leapfrog scheme. The predictor–corrector approach used here increases the computational overhead as a result of the two-stage solution. Of course, this burden is shared by the corresponding semi-implicit approach and is not due to the LT treatment. The trade-off between the twin increases in accuracy and cost will depend on the model and application.

Acknowledgements

We are grateful to Nick Byrne for his observation that the system in spectral space can be inverted analytically. This work was partly carried out while the second author was at the Atmospheric Weather Prediction Research section of Environment Canada, funded by the Visiting Fellowship programme of the Natural Sciences and Engineering Research Council of Canada, and benefitted from conversations with Janusz Pudykiewicz and Claude Girard.

Appendix

Here we present the basic theory of Laplace transforms which is relevant to this work. Further theory and applications may be found in Doetsch (1971).

Given a function $f(t)$ for $t \geq 0$, the Laplace transform (LT) is defined as

$$\widehat{f}(s) \equiv \mathfrak{L}\{f\} = \int_0^\infty e^{-st} f(t)\,\mathrm{d}t$$

The variable s is complex. It is clear that $\mathfrak{L}$ is a linear operator. In addition, the following results

may be readily found from the definition of $\mathfrak{L}$:

$$\begin{aligned} \mathfrak{L}\left\{\frac{\mathrm{d}f}{\mathrm{d}t}\right\} &= s\,\widehat{f}(s) - f(0) \\ \mathfrak{L}\{c\} &= \frac{c}{s} \qquad \text{for constant } c \end{aligned} \tag{10}$$

The inversion from a transformed function back to the original is given by the Bromwich integral

$$f(t) \equiv \mathfrak{L}^{-1}\{\widehat{f}\} = \frac{1}{2\pi i}\int_{\mathcal{C}} e^{st}\widehat{f}(s)\,\mathrm{d}s \tag{11}$$

where the contour $\mathcal{C}$ is a line parallel to the imaginary axis in the s-plane, to the right of all the singularities of $\widehat{f}$.

To remove high frequency components, we define a closed contour $\mathcal{C}^*$, the circle centred at the origin with radius ω_{c} (ω_{c} is called the cut-off frequency). We replace $\mathcal{C}$ by $\mathcal{C}^*$ in the integral in (11), yielding the modified inversion

$$f^*(t) \equiv \mathfrak{L}^*\{\widehat{f}\} = \frac{1}{2\pi i}\oint_{\mathcal{C}^*} e^{st}\widehat{f}(s)ds. \tag{12}$$

We assume that $\widehat{f}$ is meromorphic; that is, its only singularities are isolated poles. Now $f^*(t)$ contains only contributions from the poles lying within $\mathcal{C}^*$, that is, those with frequencies less than ω_{c}. Thus, the modified inversion integral (12) acts to filter high frequency behaviour.

From the definition of $\mathfrak{L}^*$ we can readily deduce the following

$$\begin{aligned} \mathfrak{L}^*\left\{\frac{1}{s}\right\} &= 1 \\ \mathfrak{L}^*\left\{\frac{1}{s^2}\right\} &= t \\ \mathfrak{L}^*\left\{\frac{1}{s^2+\omega^2}\right\} &= \frac{1}{\omega}\,H(\omega)\sin\omega t \\ \mathfrak{L}^*\left\{\frac{s}{s^2+\omega^2}\right\} &= H(\omega)\cos\omega t \\ \mathfrak{L}^*\left\{\frac{1}{s\,(s^2+\omega^2)}\right\} &= \frac{1}{\omega^2}\,(1 - H(\omega)\cos\omega t) \end{aligned} \tag{13}$$

where we have used the step function

$$H(\omega) = \begin{cases} 1\,, & |\omega| < \omega_c\,, \\ 0\,, & |\omega| > \omega_c\,. \end{cases}$$

Inversion may also be carried out numerically, by replacing this integral with a sum involving N discrete points. The resulting numerical inversion operator is denoted $\mathfrak{L}_N^*$ and is given by

$$f^*(t) \approx \mathfrak{L}_N^*\left\{\widehat{f}\right\} = \frac{1}{N}\sum_{n=1}^{N} e_N^{s_n t}\widehat{f}(s_n)\,s_n \tag{14}$$

Here, s_n are equally-spaced points around the circle $\mathcal{C}^*$ and e_N^z is the Taylor series of the exponential function, truncated to N terms. Further details of this operator are given in CL11.

Properties analogous to (13) hold for $\mathfrak{L}_N^*$: the cos and sin functions are replaced by their truncated Taylor series and the numerical filter response is given by

$$H_N(\omega) = \frac{1}{1 + (i\omega/\omega_c)^N} \,. \tag{15}$$

As $N \to \infty$, this limits to the step function $H(\omega)$.

References

[1] Asselin R. 1972. Frequency filter for time integrations. *Mon. Weather Rev.* **100**: 487–490.

[2] Beylkin G, Keiser JM, Vozovoi L. 1998. A new class of time discretization schemes for the solution of nonlinear PDEs. *J. Comput. Phys.* **147**: 362–387.

[3] Clancy C, Lynch P. 2011. Laplace transform integration of the shallow water equations. Part 1: Eulerian formulation and Kelvin waves. *Q. J. R. Meteorol. Soc.* **137**: 792–799.

[4] Clancy C, Pudykiewicz JA. 2013a. A class of semi-implicit predictor–corrector schemes for the time integration of atmospheric models. *J. Comput. Phys.* **250**: 665–684.

[5] Clancy C, Pudykiewicz JA. 2013b. On the use of exponential time integration methods in atmospheric models. *Tellus A* **65**: 20898.

[6] Daley R. 1980. The development of efficient time integration schemes using model normal modes. *Mon. Weather Rev.* **108**: 100–110.

[7] Doetsch G. 1971. *Guide to the Applications of the Laplace and Z Transforms*. Van Nostrand Reinhold

[8] Drake JB, Guo DX. 2001. *'A vorticity-divergence global semi-Lagrangian spectral model for the shallow water equations'*. Technical Report ORNL/TM-2001/216: Oak Ridge National Laboratory, Tennessee

[9] Durran DR. 1991. The third-order Adams-Bashforth method: an attractive alternative to leapfrog time differencing. *Mon. Weather Rev.* **119**: 702–720.

[10] Hack JJ, Jakob R. 1992. *'Description of a global shallow water model based on the spectral transform method'*. Technical Note NCAR/TN-343+STR. National Center for Atmospheric Research: Boulder, Colorado.

[11] Kar SK. 2012. An explicit time-difference scheme with an Adams-Bashforth predictor and a trapezoidal corrector. *Mon. Weather Rev.* **140**: 307–322.

[12] Kwizak M, Robert AJ. 1971. A semi-implicit scheme for grid point atmospheric models of the primitive equations. *Mon. Weather Rev.* **99**: 32–36.

[13] Läuter M, Handorf D, Dethloff K. 2005. Unsteady analytical solutions of the spherical shallow water equations. *J. Comput. Phys.* **210**: 535–553.

[14] Lynch P. 1991. Filtering integration schemes based on the Laplace and Z transforms. *Mon. Weather Rev.* **119**: 653–666.

[15] Williams PD. 2011. The RAW filter: an improvement to the Robert–Asselin filter in semi-implicit integrations. *Mon. Weather Rev.* **139**: 1996–2007.

[16] Williamson DL, Drake JB, Hack JJ, Jakob R, Swarztrauber PN. 1992. A standard test set for numerical approximation to the Shallow Water equations in spherical geometry. *J. Comput. Phys.* **102**: 211–224.